THE ASTROPHYSICAL JOURNAL, 300:658–668, 1986 January 15

IUE SPECTRA AND A RESULTING MODEL OF SEYFERT 2 GALAXIES[1]

GARY J. FERLAND[2]
Astronomy Department, The Ohio State University
AND
DONALD E. OSTERBROCK
Lick Observatory, Board of Studies in Astronomy and Astrophysics, University of California, Santa Cruz
Received 1985 May 3; accepted 1985 June 18

ABSTRACT

Nearly simultaneous optical and ultraviolet observations of several Seyfert 2 galaxies are presented. These, and archival data, are used to derive mean emission-line spectra and ultraviolet to X-ray spectral indices for several narrow-line objects. Both the Lyα/Hβ ratio, larger than case B, and strong C IV λ1549 suggest that the gas is ionized by a fairly hard continuum. The composite emission-line spectrum is compared with a simple photoionization model, using the observed, nearly power-law continuum, and filamentary gas clouds, a geometry which may apply to some narrow-line objects. The mean X-ray/ultraviolet continuum has a spectral index close to the value derived for Seyfert 1 galaxies and low redshift quasars and does not appear to be heavily reddened. Both suggest that an obscuring layer does not hide an underlying broad-line region, and that narrow-line objects such as Seyfert 2 and narrow-line radio galaxies are physically different from broad-line objects, at least in not having an inner broad-line region. The absence of extinction also distinguishes these classical Seyfert 2 galaxies from the narrow-line X-ray galaxies, which X-ray evidence suggests may be extinguished Seyfert 1 galaxies.

Subject headings: galaxies: Seyfert — ultraviolet: spectra

I. INTRODUCTION

The relationship between galaxies whose nuclei are characterized by broad permitted lines (the Seyfert 1 galaxies) and those which lack this component (Seyfert 2 galaxies) has been the subject of considerable speculation (cf. Osterbrock 1981*b*; Lawrence and Elvis 1982). Among the possibilities are obscuration of the broad-line region (BLR) in the Seyfert 2 class, or the intrinsic absence of dense emission-line clouds close to the nucleus. Whatever the case, both classes of galaxies have strong, narrow emission lines, and only in the case of Seyfert 2 galaxies can a reliable composite optical to ultraviolet emission-line spectrum, free of contamination by BLR components, be deduced. The optical spectra of the narrow-line regions (NLR) in the two classes of galaxies are fairly similar (see Cohen 1983), and it is quite possible that physical information about the NLR of Seyfert 2 galaxies will also have application to Seyfert 1 galaxies, as well as to quasars. The goal of this paper is to determine a mean optical to ultraviolet emission-line spectrum for Seyfert 2 galaxies, to compare these intensities with predictions of photoionization models, and to examine the ultraviolet to X-ray nonthermal continuum which ionizes this gas.

II. OBSERVATIONS

The *International Ultraviolet Explorer* (*IUE*) was used in the large-aperture (10″ × 20″), low-resolution ($\delta\lambda \approx 7$ Å) mode to observe the Seyfert 2 galaxies NGC 4388, Mrk 270, and Mrk 917 (Table 1). The short-wave portions ($\lambda\lambda$ 1200–2000) of those spectra are shown in Figure 1. Nearly simultaneous (within a few hours of the *IUE*) optical observations were obtained with the IDS spectrometer on the Lick Observatory Shane reflector.

Our goals in obtaining these observations were to measure both the composite UV–optical emission-line spectrum and the continuous energy distribution. A large (8″ × 8″) entrance aperture was used for the optical observations, both to ensure that the majority of the emission-line regions were detected and to facilitate the absolute calibration. The entrance aperture used for the satellite ultraviolet observations is still some 3 times larger than this; as a result we expect poor agreement between the Lick and *IUE* observations in regions of overlap when the source is extended. This should have little effect on the emission-line intensities since the majority of the line flux originates within a few seconds of arc of the nucleus. The different entrance apertures will almost certainly affect the continuum fluxes when starlight from the surrounding galaxy is an important contributor, however.

The continuous energy distributions, obtained by averaging the calibrated data over 50–200 Å regions chosen to be free of emission lines, are shown in Figure 2. These data are corrected for extinction by the Galaxy using the estimates of Burstein and Heiles (1982) and the extinction curve given by Seaton (1979). For comparison, Figure 2 also shows the continuum from NGC 4472, a galaxy with weak emission lines and an

TABLE 1

IUE OBSERVATIONS

Object	Image	Exposure (minutes)	Date (1984)
Mrk 917	SWP 23097	300	May 24
Mrk 917	LWP 3417	60	May 24
NGC 4388	SWP 23104	280	May 25
NGC 4388	LWP 3441	300	May 26
Mrk 270	SWP 23114	275	May 27
Mrk 270	LWP 3452	310	May 28

[1] *Lick Observatory Bulletin*, No. 1016.
[2] Guest Observer with the *International Ultraviolet Explorer*.

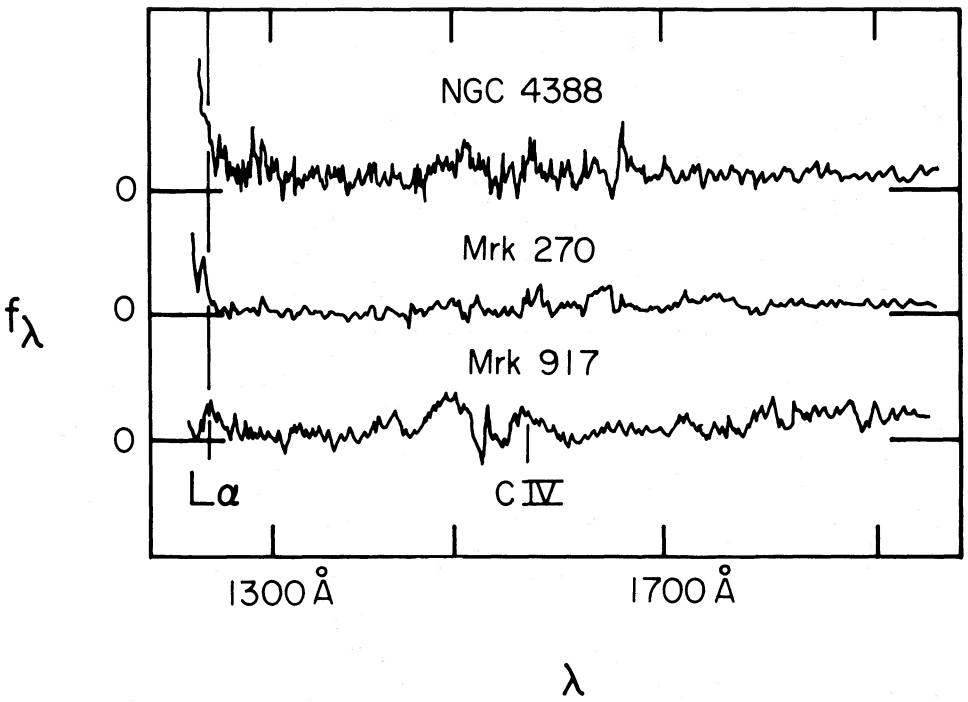

FIG. 1.—The 1200–2000 Å spectral regions are shown, uncorrected for redshift or galactic extinction. Data were corrected for the *IUE* instrument response using standard procedures and assumptions.

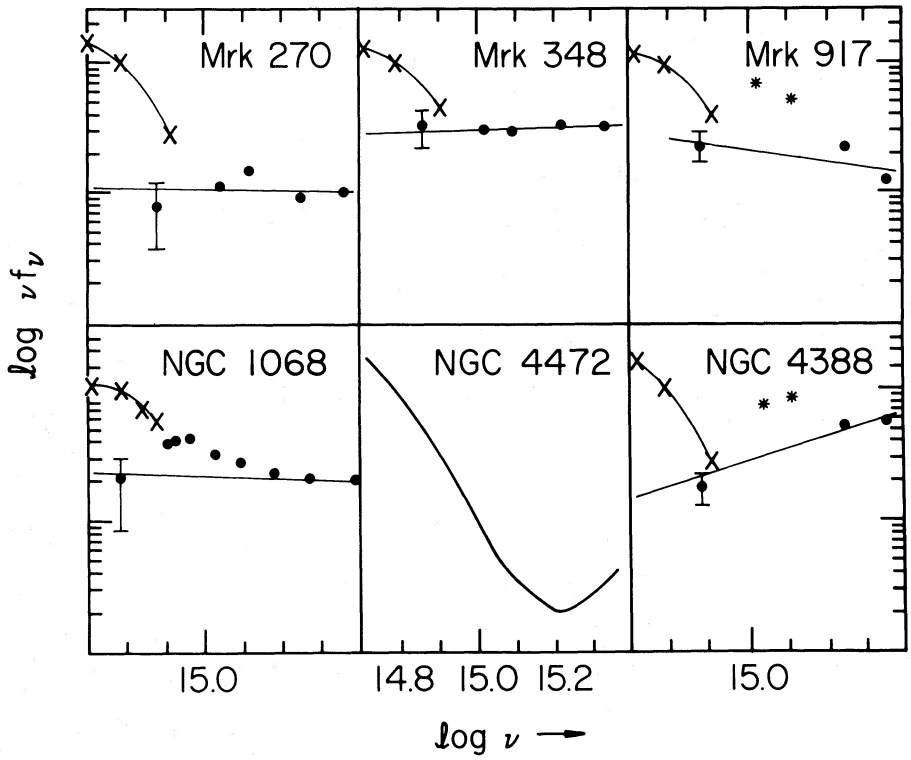

FIG. 2.—The 1400–7000 Å continua for several Seyfert 2 galaxies. NGC 4472 is a normal elliptical galaxy and is shown for comparison. Data have been corrected for reddening by the Galaxy assuming the color excesses given in Burstein and Heiles (1982). Points marked by crosses (×) are optical data taken from either Lick data or deBruyn and Sargent and are dominated by starlight. Filled circles with indicated error bars are estimated fluxes for the featureless continuum in the optical, estimated by Koski (1978) or by us using techniques similar to Koski's. Filled circles with no error bars and points indicated by an asterisk are from the referenced *IUE* data. In the case of the filled circles, the *IUE* photowrite shows that the continuum originates in a point source, while the continuum source is resolved (and probably due to starlight) in the case of the asterisks. In two cases (Mrk 917 and NGC 4388) the extrapolated continua fluxes near 3000 Å from the *IUE* and ground-based observations do not agree, almost certainly because of the different entrance apertures used in the ultraviolet and optical observations. Possible deconvolutions into stellar and nonthermal continua are indicated by the solid lines.

overall optical–UV continuum dominated by starlight. (*IUE* archival observations of NGC 4472 were combined with Lick scans to produce this energy distribution; we assume $E(B-V] = 0.06$ mag, as suggested by Burstein and Heiles.) We expect contributions from both starlight and a nonthermal featureless continuum in Seyfert 2 galaxies (see Koski 1978), and that the latter will dominate the satellite-ultraviolet continuum. We will use NGC 4472 as a rough template of the starlight to indicate those portions of the spectrum where the featureless continuum is the dominant component.

Table 2 lists intensities for the H I lines and for the stronger lines in the ultraviolet spectra. Uncertainties are typically 30% for the ultraviolet lines, unless otherwise indicated. Contamination by starlight also introduces uncertainties in our H I line fluxes (Table 2) because of the possible existence of underlying Hα and Hβ absorption lines. As discussed by Koski (1976), whether these absorption lines are significant can be assayed by examining the region near the H9, 10 lines. We discuss both problems (i.e., aperture effects and underlying absorption) as they arise in our discussions of individual cases below.

a) New Observations

i) *NGC 4388*

The optical spectrum has been discussed by Phillips, Charles, and Baldwin (1983). No emission lines were detected above the strong continuum in the *IUE* long-wave (λλ2000–3000) region, although the short-wave spectrum reveals both C IV λ1549 and Lyα emission. The strength of the latter is uncertain because of the neighboring geocoronal Lyα emission, which we tried to minimize by placing the nucleus 1″ from the center of the entrance aperture, in the direction of the dispersion. The Lyα flux listed in Table 2 is uncertain by 0.3 dex because of the weakness of the line, the strength of the geocoronal Lyα, and the possibility of underlying Lyα absorption.

The Hβ and Hα emission-line fluxes are also listed in Table 2. Our procedures and sources of uncertainties are similar to those described by Ferland and Osterbrock (1985). Hβ was measured twice, on the blue and red scans, and the quoted number is the average of the two. The contribution of Hα to the Hα, [N II] λλ6583, 6548 blend was estimated by using standard Lick programs and procedures (see Koski 1976). The stated error in the Hα flux is an estimate, judged from the range of acceptable fits, since we have no independent way to determine the uncertainty. Balmer H9, 10 absorption is weak in this galaxy, a fact which, together with the large equivalent width of Hβ (26 Å), suggests that the effects of any underlying H I absorption are relatively unimportant in this object.

Figure 2 shows the ultraviolet–optical continuum, with no correction for galactic extinction (since $E[B-V] = 0$ according to Burstein and Heiles 1982). The extrapolated optical and ultraviolet continuum fluxes do not agree well near 3000 Å ($\log \nu = 15.0$). This is undoubtedly due to the different entrance apertures used, since the *IUE* photowrite shows that the 10″ × 20″ entrance aperture was filled with starlight at wavelengths near 2500 Å (see also Thuan 1984 for a discussion of similar effects in other low-luminosity Seyfert galaxies). The photowrite also shows that both the emission lines and the continuum near 1500 Å ($\log \nu = 15.3$) comes from a point source (≤2″), however, and should reflect the featureless continuum originating in the nucleus.

In an effort to extend our detection of the featureless continuum to longer wavelengths, we have estimated its contribution to the 3900 Å region by comparing equivalent widths of some of the stronger absorption features in this galaxy with those in NGC 4472 and NGC 7331. We estimate that 45% ± 20% of the continuum at 3900 Å is not due to conventional starlight; this estimate is used to indicate a possible underlying continuum (at $\log \nu = 14.88$) in Figure 2. Our procedure for estimating this fraction is not very accurate, but we use it only to indicate the general form of the underlying nonthermal continuum; the subsequent analysis does not depend on this point.

ii) *Markarian 270*

The optical spectrum is discussed by Koski (1978). Only Lyα is detected in our *IUE* spectra (Table 2, and Fig. 1). Little H9, 10 absorption is evident in the Lick spectra, suggesting that the Hβ and Hα absorption lines in the starlight continuum are weak. Unfortunately, even weak underlying absorption lines would affect our line measurements because of the small H I equivalent widths [i.e., $W_\lambda(H\beta) = 3.4$ Å]. The Balmer intensities listed in Table 2 have uncertainties estimated in the usual way, but increased by an additional factor of 2 because of the possibility of underlying absorption. Koski (1978) lists an Hβ flux some 34% larger than we measure (we find 2.27×10^{-14} ergs cm^{-2} s^{-1}), perhaps because of differences in aperture or calibration. Figure 2 shows the UV–optical energy distribution after correction for $E(B-V) = 0.02$ mag. Our new data, as well as Koski's (1976) analysis, suggest that ~20% of the continuum near 3900 Å is not starlight.

TABLE 2

EMISSION-LINE INTENSITIES[a]

Object	Lyα	C IV λ1549	C III] λ1909	Mg II λ2798	Hβ	Hα
NGC 4388	1.2(−13):	8.0(−14)	≤1.7(−14)	<2.2(−14)	7.0 ± 0.9(−14)	3.6(−13)
Mrk 270	2.0(−13)	≤7.7(−14)	<4(−14)	≤1.3(−14)	1.7 ± 0.6(−14)	1.1(−13)
Mrk 917	≤8.4(−14)	<3.2(−14)	<4.4(−14)	...	2.3 ± 0.3(−14)	1.4(−13)
Mrk 3	6.3 ± 0.1(−13)	1.9 ± 0.2(−13)	1.0 ± 0.2(−13)	1.6 ± 0.2(−13)	3.1(−13)	1.6(−12)
Mrk 78	7.0(−13)	2.(−13):	2.(−13):	...	4.9(−14)	2.6(−13)
Mrk 348	5.1(−13)	1.2(−13)	3.4(−14)	1.8(−14):	2.8(−14)	9.9(−14)
NGC 1068	7.6(−12)	4.8(−12)	1.5(−12)	8.3(−13)	1.6(−12)	8.7(−12)
3C 98	<3(−14)	<3(−14)	<3(−14)	...	2.6(−15)	1.7(−14)
3C 192	1.1(−13)	<3(−14)	<3(−14)	...	4.2 ± 0.6(−15)	1.5 ± 0.2(−14)
3C 223	3.3(−14)	<2(−14)	<2(−14)	...	3.6 ± 0.6(−15)	1.6 ± 0.2(−14)
3C 317	<5.6(−14)	<2(−14)	<2(−14)	...	5.2(−16)	4.3(−15)
3C 405	<6.1(−14)	<5(−14)	<3(−14)	...	1.2(−14)	7.9(−14)

[a] Intensities in units of ergs s^{-1} cm^{-2}. The number in parentheses is the exponent; $3(-10) \equiv 3 \times 10^{-10}$.

iii) *Markarian 917*

Lyα was not detected in our shortwave scan. The Lick scan reveals moderately strong H9, 10 absorption. Accordingly, following a suggestion by W. C. Keel, we have attempted to correct for underlying Hβ and Hα absorption by assuming that the galaxy spectrum is similar to that of NGC 7331. This correction for absorption increases the Hβ flux from $1.8 \pm 0.2 \times 10^{-14}$ to $2.3 \pm 0.3 \times 10^{-14}$ ergs s^{-1} cm^{-2}. The correction to Hα is considerably smaller because of its greater emission-line equivalent width.

The continuous energy distribution (Fig. 2) has not been corrected for reddening in our Galaxy, which should be small in the direction of Mrk 917. The contribution of the featureless continuum to the observed continuum near 3900 Å was estimated as above. Both the shape of the energy distribution and the size of the continuum source in directions perpendicular to the dipersion suggest that starlight is the dominant contributor to the continuum longward of 2500 Å, and that a nonthermal source is the dominant contributor shortward of 2500 Å.

b) Archival Observations

In addition to the new observations presented above, we have examined the *IUE* data base for previous observations of Seyfert 2 galaxies. Table 3 lists the scans we have examined, and Table 2 gives the measured line fluxes. The ultraviolet and optical data discussed in this section are not simultaneous, but light travel time arguments suggest that the emission lines should be constant. It is not known whether the featureless continuum is highly variable in typical Seyfert 2 galaxies.

i) *Markarian 3*

The ultraviolet and optical spectra have been discussed by Malkan and Oke (1983), and the optical spectrum by Koski (1978) and by Briggs *et al.* (1980). The flux in Hβ as measured by Malkan and Oke and by Koski disagree by some 50%, perhaps because of aperture effects (Malkan and Oke use somewhat larger apertures). We adopt Hα and Hβ fluxes from Malkan and Oke, and ultraviolet fluxes which are the average of our independent measurements of the archival data, and those of Malkan and Oke. The ultraviolet continuum in Mrk 3 was too weak to be reliably measured.

ii) *Markarian 78*

The shortwave spectrum obtained by C. C. Wu in 1979 is discussed by Wu, Boggess, and Gull (1983). Lyα is easily measured, and weak C IV λ1549 and C III] λ1909 are evident. Optical spectrophotometry is presented by Koski (1978) and deBruyn and Sargent (1978). These independent optical observations do not agree well (again perhaps because of aperture effects). We have adopted the absolute Hβ flux of deBruyn and Sargent because of their larger entrance aperture, and the Balmer decrement listed by Koski because of his better resolution and line deconvolution.

TABLE 3

ARCHIVAL DATA

Object	Image	Exposure (minutes)	Date[a]
Mrk 3	SWP 13738	428	1981 107
Mrk 3	LWR 10199	199	1981 83
Mrk 78	SWP 3958	180	1979 21
Mrk 348	SWP 14349	330	1981 179
Mrk 348	LWR 11163	286	1981 209
NGC 1068	SWP 16441	40	1982 58
NGC 1068	LWR 12687	25	1982 58
3C 98	SWP 4256	90	1979 45
3C 317	SWP 6330	400	1979 242
3C 405	SWP 4257	185	1979 45

[a] Date in form: year, day of year.

iii) *Markarian 348*

Both longwave and shortwave spectra were obtained in 1981, and Lyα, C IV λ1549, C III] λ1909, and Mg II λ2798 emission lines are easily detected. DeBruyn and Sargent (1978) and Koski (1978) present optical data. The line fluxes are in relatively good agreement (20%), while the continua disagree by some factor of 2, presumably because of aperture effects. We use the optical data of Koski (1978) for the Balmer line fluxes listed in Table 2 and take the continuous energy distribution from deBruyn and Sargent. The UV continuous energy distribution is dominated by a flat nonstellar continuum.

iv) *NGC 1068*

The ultraviolet and optical spectrum is discussed by Neugebauer *et al.* (1980). Intensities of ultraviolet lines have been independently measured from the listed scans (Table 3). The Balmer line intensities measured by Neugebauer *et al.* and by Koski do not agree well (almost certainly because of aperture effects, since the emission-line regions of this galaxy are known to be extended; Walker 1968), and we adopt the values listed by Neugebauer *et al.* because of their larger entrance aperture. The optical continuous energy distribution is from deBruyn and Sargent.

v) *Narrow-Line Radio Galaxies 3C 98, 3C 317, and 3C 405*

Shortwave spectra were reprocessed using the most recent *IUESIPS* extraction procedure, especially for our use. Lyα was not detected on any scan. The optical data are from Cohen and Osterbrock (1981), Costero and Osterbrock (1977), and Osterbrock and Miller (1975).

vi) *Narrow-Line Radio Galaxies 3C 192 and 3C 223*

Combined optical–ultraviolet spectra are discussed by Ferland and Osterbrock (1985). Only Lyα is detected in the ultraviolet spectra.

vii) *Radio Galaxy PKS 2158−380*

Data over a broad range of wavelengths were presented by Fosbury *et al.* (1982). We regret that we overlooked this paper, which contains the first reported detection of Lyα in a narrow-line radio galaxy, in our discussion of 3C 192 and 3C 223 (Ferland and Osterbrock 1985).

III. A MEAN SEYFERT 2 SPECTRUM

The ultraviolet and optical emission lines detected on our spectra represent a wide range of ionization and excitation potentials. As a result, their relative intensities offer clues to the physical conditions in the emitting regions which cannot be obtained from optical data alone. Unfortunately, the reddening correction may be large, and certainly is poorly determined; it must be made before the emission-line measurements can be interpreted. In this section we estimate the reddening using the Balmer and Lyman decrements, and then obtain a mean emission-line spectrum.

Gaskell and Ferland (1984) noticed that the predicted H I spectra of many NLR models tend to lie in a narrow band on an Hα/Hβ/Lyα diagram. The theoretical underpinning, as well as an application to narrow-line radio galaxies, was discussed

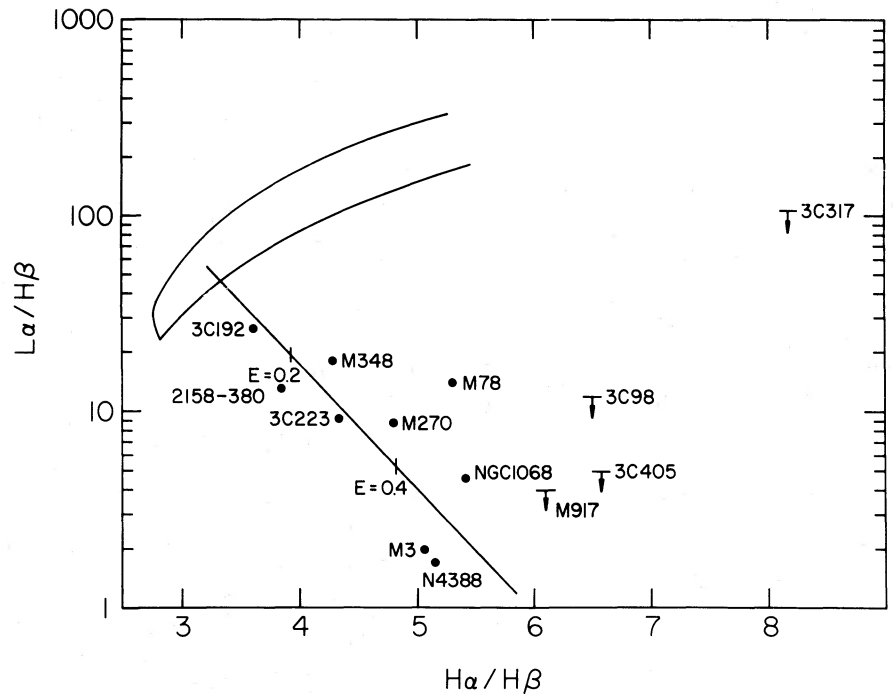

FIG. 3.—Range of permitted Lyα/Hβ and Hα/Hβ ratios is shown as the arced lines above. Arguments summarized in the text suggest that the intrinsic H I spectra of narrow-line gas should lie within the indicated bounds. The heavy straight line indicates a reddening track away from a region near the center of the allowed H I spectrum. Hashmarks indicate reddenings of $E(B-V) = 0.2$ and 0.4 mag. Points indicate positions of various narrow-line objects. Upper limits are indicated by the downward pointing arrow.

by Ferland and Osterbrock (1985). Basically, the H I spectrum of the low-density gas in an active galactic nucleus can differ from the case B recombination spectrum because of a contribution from collisional excitation in warm neutral regions (Netzer 1982; Halpern 1982). The main effect is to amplify the strength of Hα, and especially of Lyα, by amounts which are related to each other by a ratio of excitation cross sections. As a result, the Lyman and Balmer decrements can be predicted as functions of each other. Uncertainties enter because of the range of temperatures and densities likely to be encountered, but for reasonable values of the electron temperature ($8000 < T < 12{,}000$ K), and the full range of densities, the H I spectrum should lie between the bounds set by the equations (Ferland and Osterbrock 1985)

$$I(\mathrm{Ly}\alpha)/I(\mathrm{H}\beta) < 34.3 + 165[I(\mathrm{H}\alpha)/I(\mathrm{H}\beta) - 2.84] ,$$

$$I(\mathrm{Ly}\alpha)/I(\mathrm{H}\beta) > 23.3 + 52.2[I(\mathrm{H}\alpha)/I(\mathrm{H}\beta) - 2.84] .$$

This allowed range of H I spectra, together with a reddening track away from the center of the expected region (assuming the extinction curve of Seaton 1979), are shown in Figure 3. The H I measurements given in Table 2 are also shown. Apparently, the range in reddening implied by the Lyman and Balmer decrements is large, with some values as great as $E(B-V) = 0.5$ mag. (This assumes, of course, that the reddening law characterizing the material responsible for the extinction of the emission from the NLR gas is similar to the mean reddening law for our Galaxy adopted by Seaton 1979. We are forced to make this assumption by the lack of any information on which to base a better assumption.) The intrinsic H I decrements of most of the observed objects is typically $I(\mathrm{H}\alpha)/I(\mathrm{H}\beta) \approx 3.1$, $I(\mathrm{Ly}\alpha)/I(\mathrm{H}\beta) \approx 55$, steeper than case B, in agreement with recent photoionization models (see Pequignot 1984).

A major goal of this work is to deduce a mean or composite emission-line spectrum for Seyfert 2 galaxies. We use the mean spectrum given by Cohen and Osterbrock (1981) for stronger optical lines and supplement this list with ultraviolet observations, and other optical data. Table 4 lists line intensities for some of the stronger ultraviolet lines, measured from the archival data listed in Table 3. All intensities are given relative to Lyα, and for each object there are two entries, one for the observed line ratios, and the second for the ratios corrected for the color excess given in the last column of Table 4 (deduced from the observed H I decrement and its displacement from the center of the allowed range in Fig. 3). The bottom row of Table 4 gives the mean line ratio (after correcting for reddening) and

TABLE 4

ULTRAVIOLET LINES

Object	C IV λ1549 / Lyα	C III] λ1909 / Lyα	Mg II λ2798 / Lyα	$E(B-V)$
Mrk 3	0.27	0.19	0.24	0
	0.14	0.092	0.052	0.48
Mrk 78	0.29:	0.29:	...	0
	0.18	0.17	...	0.35
Mrk 348	0.24	0.067	0.035	0
	0.17	0.047	0.016	0.24
NGC 1068	0.63	0.20	0.11	0
	0.35	0.11	0.029	0.42
Mean	0.21 ± 0.09	0.10 ± 0.05	0.032 ± 0.018	

TABLE 5

COMPOSITE SPECTRUM

Line	I_{obs}	$I_{predicted}$
H I λ1216	55 ± 20	32.6
H I 2ν	...	3.06
H I λ4861	1.00	1.00
H I λ6563	3.1 ± 0.1	2.91
He I λ5876	0.13 ± 0.06	0.17
He II λ4686	0.29 ± 0.1	0.18
C II] λ2326	...	1.18
C III] λ1909	5.5 ± 3.7	1.35
C IV λ1549	12 ± 8	1.04
[N I] λ5199	0.15 ± 0.09	0.07
[N II] λ6583	2.9 ± 1.0	2.56
[O I] λ6300	0.57 ± 0.2	0.85
[O II] λ3727	3.2 ± 1.7	2.51
λ7325	...	0.62
[O III] λ5007	10.8 ± 3.0	7.11
λ4363	0.21 ± 0.1	0.11
O VI λ1034	...	0.16
[Ne III] λ3869	1.4 ± 0.4	0.98
[Ne III] 15.6μ	...	1.63
[Ne V] λ3426	1.2 ± 0.2	0.09
Mg II λ2798	1.8 ± 1.5	2.32
Si II λ2336	...	0.20
Si III λ1895	...	0.18
Si IV λ1397	...	0.08
[S II] λ6716	1.5 ± 0.5	0.52
λ6731		0.85
λ4074	0.30 ± 0.2	0.50
[S III] λ9532	...	1.66
[A III] λ7136 :	0.24 ± 0.07	0.23
[A III] 9μ	...	0.15
[Fe II] F7	<0.1	1.62
[Fe II] UV3	...	2.43
[Fe V] λ3892	<0.1	0.14
[Fe VI] λ5177	<0.1	0.13
[Fe VII] λ6087	0.10 ± 0.05	0.02
[Fe X] λ6375	0.04 ± 0.04	0.002

the scatter about this mean. Finally, Table 5 gives the composite intrinsic UV–optical spectrum, taken from Cohen and Osterbrock (1981), Table 3, and supplemented by some infrared lines from Malkan and Oke's (1982) measurements of Mrk 3. Note that only the Seyfert 2 galaxies which show the high-ionization lines [Fe VII] λ6087 and [Fe X] λ6375 were included in the respective average relative intensities of these two lines; the table is thus somewhat biased toward high ionization compared with the *average* Seyfert 2. The dispersion in emission-line intensities is also given and is largely due to scatter in the intrinsic relative intensities.

IV. THE NONTHERMAL CONTINUUM

Are Seyfert 2 galaxies really active galactic nuclei (which we here define as nuclei with a photoionizing featureless continuous spectrum extending to high energies), and why do they lack broad permitted lines? Veron *et al.* (1980), Lawrence and Elvis (1982), and Mushotzky (1982) have suggested that the absence of BL emission is an obscuration effect. In their models Seyfert 1 and 2 galaxies are similar; the latter are supposed to be oriented so that emission from the inner BLR is extinguished by material lying between the broad- and narrow-line regions. This interpretation is supported by the fact that Keel (1980) showed that Seyfert 1 galaxies tend to have more nearly face-on orientations than average spirals, while Lawrence and Elvis (1982) found that X-ray selected narrow-line galaxies (which are sometimes said to be Seyfert 2 galaxies) tended to be more nearly edge-on, with soft X-ray evidence for intervening absorption. Another possibility is that Seyfert 2 galaxies have many properties in common with broad-line objects, but simply lack a broad-line region.

A comparison between the ultraviolet to X-ray continua in Seyfert 2 galaxies and broad-line galaxies may be able to decide between the various possibilities. Several Seyfert 2 galaxies have been detected by the *Einstein Observatory* as soft X-ray sources (Table 6), and we combine *IUE* data with IPC data to determine a mean value of the ultraviolet to X-ray spectral index. The fact that the slope thus found is similar to that for quasars and Seyfert 1 galaxies suggests that Seyfert 2 galaxies are close relatives, and that the interstellar extinction may not be sufficient to hide an inner broad-line region.

Narrow-line radio galaxies and Seyfert 2 galaxies have similar emission-line spectra (see above and Cohen and Osterbrock 1981), so we combine X-ray observations of both to improve the statistics. Table 6 gives the galaxy name (col. [1]), the flux at 2500 Å (col. [2], these have been corrected for reddening due to our Galaxy but *not* for the reddening indicated by the H I line ratios), and the soft X-ray flux, taken from Neugebauer *et al.* (1980; NGC 1068), Kriss, Canizares, and Richert (1980; Mrk 78, Mrk 348, Mrk 507), Ulvestad and Wilson (1983; Mrk 573), and Fabbiano *et al.* (1984; 3C 184.1, 3C 433). The deduced value of the 2500 Å–2 keV spectral index α (defined such that $f_\nu \sim \nu^{-\alpha}$) is given in the fourth column. Those objects which have an colon next to the 2500 Å flux were not measured directly with *IUE*, but rather have 2500 Å fluxes which are extrapolations from the optical featureless continuum measured by Koski (1978), assuming a spectral index of 1.4. The frequency of the X-ray flux for NGC 1068 is 0.3 keV rather than 2 keV, as noted by Neugebauer *et al.* (1980).

Table 6 also lists the mean ultraviolet to X-ray spectral index for radio-loud quasars and radio-quiet QSOs (Zamorani *et al.* 1981). The mean spectral index of our sample of Seyfert 2 galaxies and narrow-line radio galaxies (NLRGs) ($\langle\alpha\rangle = 1.4 \pm 0.2$) falls near the center of the range measured for the larger sample of broad-line objects, suggesting a similar general shape for the ionizing continuum. That the continua in Seyfert 2 galaxies may indeed follow a simple power-law is suggested by the fact that the mean optical spectral index mea-

TABLE 6

OPTICAL X-RAY CONTINUA

Object (1)	νf_ν (2500 Å) (2)	νF_ν (2 keV) (3)	α_{ox} (4)
NGC 1068	1.4(−10)	2.1(−11)[a]	1.46
Mrk 78	3.3(−12)	5.8(−14)	1.69
Mrk 348	3.6(−12)	2.4(−13)	1.46
Mrk 507	1.4(−12):[b]	7.0(−13)	1.12
Mrk 573	9.4(−13):	4.5(−13)	1.12
3C 184.1	1.5(−12):	1.3(−13)	1.41
3C 433	1.4(−12):	9.0(−14)	1.46
Mean			1.39 ± 0.20
Radio-loud[c]			1.27 ± 0.06
Radio-quiet[c]			1.46 ± 0.06
Koski α_{opt}[d]			1.32 ± 0.6

[a] Soft X-ray point at 0.3 keV.
[b] Colon indicates 2500 Å continuum extrapolated from optical.
[c] Indices for broad-line objects taken from Zamorani *et al.* 1981.
[d] Mean spectral index for optical featureless continuum, taken from Koski 1976.

sured by Koski (1978) in his sample of Seyfert 2 galaxies and NLRGs (including only those objects in which the featureless continuum contributed more than 25% of the total flux at 4800 Å) is $\langle\alpha\rangle = 1.3 \pm 0.6$, close to the ultraviolet to X-ray spectral index. These averages suggest that a single power law, with a spectral index of 1.4 and extending from the optical to beyond 2 keV, may be a fair approximation to actual Seyfert 2 continua.

Are Seyfert 2 galaxies heavily reddened—in particular, reddened enough to hide an inner broad-line region? The fact that the spectral index is close to that obtained for active nuclei (with only a correction for reddening due to our Galaxy) suggests that the line of sight to the continuum source is not heavily extinguished. Unless the dust is distributed in such a way as to extinguish only the BLR and not the continuum source, the conclusion is that these objects simply lack a BLR. The original suggestion that narrow-line galaxies are obscured Seyfert galaxies was made to account for some properties of the class of narrow-line X-ray galaxies, which are sometimes referred to as Seyfert 2 galaxies. It is important to remember that "classical" Seyfert 2 galaxies do have brilliant, stellar appearing nuclei; these objects are *not* the same as narrow-line X-ray galaxies, which tend to be edge-on spirals, do show evidence for soft X-ray and optical absorption, and could well be cloaked Seyfert 1 galaxies (Keel 1980; Lawrence and Elvis 1982; Mushotzky 1982). Narrow-line X-ray galaxies and classical Seyfert 2 galaxies are selected by different criteria, have different optical properties, and should not be confused with each other.

Although we do not see evidence of the strong extinction needed to hide the inner regions of a Seyfert 1 galaxy from our view, the reddening of the NLR gas obtained in § II is in some cases substantial. However, it does not seem likely that the featureless continuum is reddened even by this much. If the ultraviolet continua shown in Figure 2 (which have been corrected for galactic reddening only) were to be dereddened by the amount indicated by the H I spectrum, then each galaxy would have a continuum with a slope which was a function mainly of the assumed reddening, rather than the fairly uniform, flat slopes shown in Figure 2. In other words, if it were proper to correct the observed continua for the reddening deduced from the lines, then the flat continua shown in Figure 2 result from a coincident correlation between different reddenings and continua, which conspired in such a way as to produce similar observed continua. Similar arguments for continuum reddening being smaller than line reddening were made by Osterbrock and Miller (1975) and Costero and Osterbrock (1977) in their studies of NLRG. Apparently, the absorbing dust which extinguishes the lines is associated with the NLR gas, and does not cover the line of sight from Earth to the continuum source.

V. COMPARISON WITH PHOTOIONIZATION MODELS

One goal in observing these galaxies was to deduce properties of the NLR gas by comparing the mean emission-line spectrum with predictions of photoionization models. A photoionization model is parameterized by (i) the shape and luminosity of the ionizing continuum, (ii) the density profile of the gas, and (iii) the chemical composition of the gas. We make the simplest possible assumptions concerning all these parameters.

a) Spatial Structure

Model spatial structures of Seyfert 2 emission-line gas fall into three broad categories. The simplest is characterized by a single density and distance from the source of ionizing radiation. Such an approach has been taken by, among others, Ferland and Netzer (1983), Halpern and Steiner (1983), and Stasinska (1984). Although it may have heuristic value, such a model does not survive careful observational scrutiny. Problems such as the existence of inhomogeneities and the fact that lines of different species have different widths rule out such a simple model for the NLR. For instance, often the [S II] $\lambda\lambda$6716/6731 line ratio indicates electron densities near $N_e \sim 10^3$ cm^{-3}, while [O III] (λ4959 + λ5007)/λ4363 indicates densities nearer 10^5 cm^{-3} if the gas is photoionized (see Cohen and Osterbrock 1981). Single-component models also cannot account for correlations between line width and ionization potential or critical density (see DeRobertis and Osterbrock 1984; Filippenko and Halpern 1984).

A second possible geometry, which can account for the observed range of both ionization and density, is analogous to the situation in some planetary nebulae or in H II regions. Here the gas has condensed into small filaments, which are individually optically thin to the ionizing continuum, but which lie over a large range in radii (see MacAlpine 1972). If velocity is correlated with radius in some manner (as in planetary nebulae), then lines formed at different radii will have different widths. Furthermore, if the gas density obeys some $N(r)$ law, such as a power law, then inhomogeneities can be modeled simply, and there will be a line width versus ionization potential correlation. We will discuss such a simple model in detail below.

The last (and unfortunately for simple theories, a likely) situation is one in which gas exists over a wide range in radius, but has coalesced into small components which are each optically thick to the ionizing continuum. Such a geometry is illustrated by Osterbrock (1984). In this case the density, dimensions, and possible shadowing effects all influence the resulting emission. Although the density may be a simple function of radius (if, for example, the clouds are in pressure equilibrium with a surrounding medium, see Krolik and Vrtilek 1984), situations in which the gas has a mixture of densities at a given radius (either because it is not confined or has not had time to equilibiate with its surroundings) can be envisioned. First steps in calculating optically thick, $N = f(r)$, models have been taken by Carroll and Kwan (1983) and Contini and Aldrovandi (1983).

The width of the [O I] λ6300 line offers a test of whether individual clouds are optically thin or thick to the ionizing continuum. In an optically thin geometry neutral oxygen is found only near the H^0–H^+ ionization front, which occurs at the outer edge of the emission-line region. If velocity decreases with radius, then the [O I] line will be among the sharpest. If, rather, individual clouds are optically thick and H ionization fronts occur in each, then some [O I] emission will be formed even in the innermost clouds, and [O I] λ6300 may be among the broadest emission lines. The former is indeed the case in the NLR of the high-ionization Seyfert 1 galaxy III Zw 77 (Osterbrock 1981*a*), as well as in some of the galaxies studied by DeRobertis and Osterbrock (1984; Mrk 533 is an example). Many other galaxies are encountered in which the [O I] line is among the broadest (Filippenko and Halpern 1984; DeRo-

bertis and Osterbrock 1984; NGC 7213 is an example). Evidently, both geometries may be encountered in nature (see also Whittle 1985).

We model the gas as a simple optically thin filamentary geometry, motivated by the simplicity of such a model, by the fact that its implications have not been carefully examined, and because it may have application to some active nuclei.

b) *The Chemical Composition*

The chemical composition is an important ingredient in any model. Koski (1978) found a nearly cosmic He/H ratio (~ 0.1) in his sample of Seyfert 2 galaxies and NLRG, and Osterbrock and Miller (1975) found roughly solar abundances in the NLRG Cyg A. Here we estimate the electron temperature and C/O ratio for our composite spectrum after making certain assumptions about the electron density and oxygen abundance.

We first estimate the electron temperature. It is possible to relate T_e to the [O III] $\lambda 4363$ and He I $\lambda 5876$ intensities in a way which is only weakly sensitive to the O/He abundance ratio, if the density is below the critical density for O^{+2} ^1S ($N_c \approx 2 \times 10^7$ cm^{-3}). (This assumption seems reasonable, although it would come as no great surprise if denser regions also contribute to the NLR.) Assuming standard rates, and assuming that He I $\lambda 5876$ is formed by recombination, and that O^{+2} fills the He^+ zone (an assumption supported by model calculations), we find

$$t = \frac{6.176}{11.426 + \ln [I(5876)/I(4363)] + \ln [O^{++}/He^+] + 0.6/t},$$

suggesting $t = T_e/10^4$ K $= 1.1$ (± 0.2 dex). The stated error includes a ± 0.5 dex uncertainty in the O/He ratio, which we take to be 4×10^{-3} (this uncertainty in the O/He ratio includes the full range of oxygen abundances found in H II regions by Pagel and Edmunds 1981), as well as an additional uncertainty due to changes in the ^1S excitation rate due to variation in the population of ^1D (which is thermalized at densities greater than $\sim 10^6$ cm^{-3}).

Our mean spectrum includes lines of C, and these are consistent with roughly solar abundances. The abundance of C relative to O is related to the intensities of the UV C III] and C IV lines, relative to [O III] $\lambda 4363$, by

$$\frac{C^{+2} + C^{+3}}{O^{+2}} = 83\, e^{-1.34/t} \frac{I(1909)}{I(4363)} + 463\, e^{-3.09/t} \frac{I(1549)}{I(4363)},$$

where we again assume that the density of the emitting region is less than $N_c(^1S)$, and a temperature of 11,000 K $\pm$ 5000 K. (These ratios of emission-line intensities are advantageous because the Boltzmann factors nearly cancel, resulting in only a weak temperature dependence.) The line ratios of Tables 2, 4, and 5 suggest $(C^{+2} + C^{+3})/O^{+2} \approx 1$. Both photoionization models and ionization potential considerations suggest that, while O^{+2} is confined to the He^+ zone, C^{+3} can be found in both the He^+ and He^{+2} zones. As a result this expression is an upper limit to the actual C/O ratio, and the estimate is consistent with roughly solar C/O. (We assume that dust plays no role in destroying the ultraviolet lines. The validity of this assumption is open to question, especially since it is known that dust selectively destroys ultraviolet resonance lines in some planetary nebulae; see Harrington, Lutz, and Seaton 1981. We assume a dust-free environment throughout the following discussion.)

c) *The Ionizing Continuum*

Both the relatively strong ultraviolet carbon lines and the large Lyα/Hβ ratio deduced in § III suggest that the gas is ionized by a fairly energetic continuum, a suspicion confirmed by the presence of such lines as [Fe X] $\lambda 6375$ and [Fe VII] $\lambda\lambda 5721$, 6087. We use a simple power-law continuum, with spectral index $\alpha = 1.4$, and with a luminosity normalized to produce the observed 0.5–4.5 keV luminosity of 10^{42} ergs s^{-1} which is characteristic of the classical Seyfert 2 galaxies in the Lawrence and Elvis (1982) sample.

d) *The Envelope Structure*

We set the envelope structure with as few assumptions as possible. As outlined above, the best evidence suggests that the NLR gas has a range of densities and ionization. Ideally, one should use a fully self-consistent model for the origin and evolution of this gas to make *ab initio* predictions concerning its structure, and some steps in this direction have been taken (Carroll and Kwan 1983; Krolik and Vrtilek 1984). Here we limit ourselves to a simple power-law density distribution with a uniform volume filling factor. If we write the density as $N(r) \sim r^{-\beta}$, we have the limits that β must be less than 2 (which would correspond to an ionization parameter constant with radius, in the absence of absorption) but that β must be greater than 0 (which would be a constant density model). We use $\beta = 1$, with mainly simplicity to recommend it [i.e., $N(r) \sim 1/r$].

The density at the inner radius is set by the constraint that iron is sometimes 9 times ionized ([Fe X] $\lambda 6375$ is included in the mean composite spectrum). Expressed as a limit to the ionization parameter (U = ionizing photon density/free electron density), this corresponds to $\log (U) > -0.5$. Other limits are that $N_e \approx 10^3$ cm^{-3} in the [S II] $\lambda\lambda 6716$, 6731 emitting region, and $\sim 10^5$ cm^{-3} in much of the [O III] region. For our adopted continuum and model, the inner radius and density are $r = 10^{17}$ cm and $N_H = 5 \times 10^7$ cm^{-3}.

The filling factor ϵ for the NLR gas is the only remaining free parameter. This is set by matching the observed [O III] $\lambda 5007$/[O II] $\lambda 3727$ ratio. Basically, the dependence on ϵ occurs because smaller values of the filling factor tend to make the model more extended, which accentuates the importance of the outer, low-ionization regions. Smaller values of ϵ produce smaller [O III] $\lambda 5007$/[O II] $\lambda 3727$ ratios. Typically, $\epsilon \approx 10^{-5.5}$ is indicated. This filling factor produces outer radii and densities of $r \approx 10^{21}$ cm and $N_e \approx 10^3$ cm^{-3}, respectively. (The electron density in outer regions of the model is lower than the hydrogen density because the gas is only partially ionized.)

The last column of Table 5 gives the emission-line spectrum predicted by this model. With few exceptions, the lines are in general agreement with observed values. In particular, we stress that we have not "fine tuned" the model, for instance by making slight changes to the chemical composition or ionizing continuum. The three outstanding successes are observable [Fe X] $\lambda 6365$ emission, an [O III] $\lambda 5007/\lambda 4363$ ratio (55.4) which indicates $N_e \approx 4 \times 10^5$ cm^{-3} if $T_e = 10^4$ K, and an [S II] doublet ratio ($\lambda 6716/\lambda 6731 = 0.61$) which indicates $N_e = 2000$ cm^{-3}. An outstanding deficiency is the nearly case B H I spectrum, caused by the fact that the neutral regions of this simple model have relatively low densities and temperatures. As a result, regions of the model where hydrogen is neutral produce little collisionally excited Lyα.

Figure 4 shows the thermal and ionization structure of this

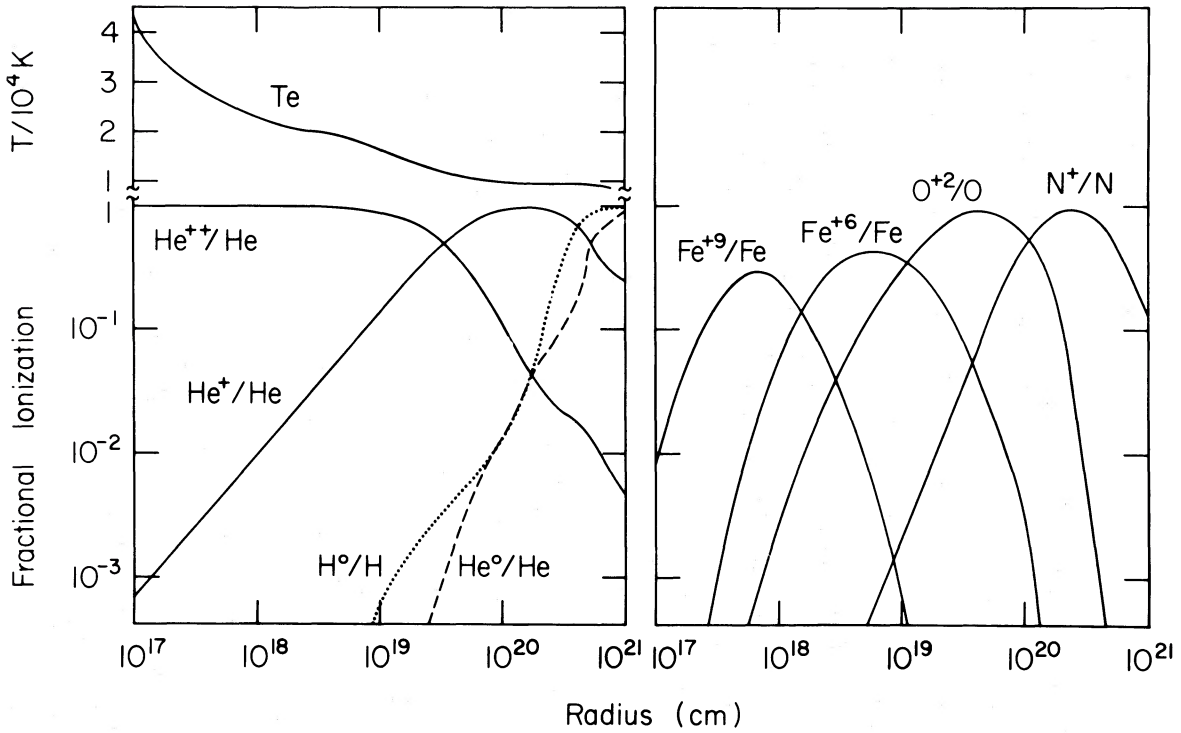

FIG. 4.—Ionization and thermal structure of the model narrow-line region described in the text is shown.

model. It extends over a factor of $\sim 10^4$ in radius, suggesting that the various lines would in fact have different widths, depending on their mean positions of formation and the velocity field. One would, of course, need a specific model for the potential of the nucleus and the wind before detailed predictions concerning the observed lines widths could be made.

Is the central source of ionizing radiation, which we model as a single power law, sufficient to power the emission-line regions? A simple comparison between the power available in ionizing radiation and the emission-line luminosities may provide an answer (cf. Osterbrock and Parker 1965; Neugebauer *et al.* 1980). The average soft X-ray luminosity of the classical Seyfert 2 galaxies detected in the Lawrence and Elvis (1982) sample is $L_X = 10^{42}$ ergs s^{-1}, and the mean Hβ luminosity is 6×10^{40} ergs s^{-1} (± 0.7 dex). For comparison, our model, which has the same soft X-ray luminosity (corresponding to a total luminosity in ionizing radiation of $\sim 7 \times 10^{42}$ ergs s^{-1}), produces an Hβ luminosity of 4.5×10^{40} ergs s^{-1} if the gas fully covers the source of radiation. Another test is the ratio of the luminosity in [O III] λ5007 to the soft X-ray luminosity, which Lawrence and Elvis find to be about equal. For full coverage, the model predicts this ratio to be $L([\text{O III}])/L_X \approx 0.34$, nearly a factor of 3 too small. Both problems would be much worse if the gas were patchy and did not fully cover the continuum source.

Is there an energetics problem in Seyfert 2 galaxies? Possibly the continuum is not as simple as we assume; for instance, Netzer (1985) has suggested that the continuum in broad-line objects may actually be rising at wavelengths shortward of the Lyman limit. Such a continuum would increase the total power in ionizing radiation without significantly affecting the soft X-ray or ultraviolet luminosities. Shocks (see Daltabuit, MacAlpine, and Cox 1978) or fast particles (see Ptak and Stoner 1973) could also play roles. Another possibility is that starlight contributes to the ionization of the outer regions of the NLR. A population of early-type stars within a few hundred parsecs of the nucleus would increase the ionization of the outer regions of the model, and observational evidence for a nuclear disk of young stars in NGC 1068 has been summarized by Weedman and Huenemoerder (1985). Spatially resolved soft X-ray and satellite ultraviolet observations would be needed to decide among the various possibilities.

VI. CONCLUSIONS

The observational evidence suggests that Seyfert 2 galaxies are active galaxies which for some reason lack an inner broad-line region. This is supported by the fact that Seyfert 2 galaxies appear to have nearly the same X-ray to ultraviolet flux ratio as Seyfert 1 galaxies, quasars, and QSOs. This argues for similar origins for the featureless continuum in both broad-and narrow-line objects. Color excesses between $E(B-V) = 0.2$ and 0.6 mag are deduced from the emission-line spectra, an amount of extinction insufficient to hide an inner broad-line region. The evidence suggests that the line of sight to the continuum source does not include as much extinction as that to the emission-line regions, perhaps an indication that the absorbers are patchy or associated with the emitting clouds. These considerations suggest that Seyfert 2 nuclei lack a broad-line region because they do not have one, rather than because an existing BLR is hidden from view by an absorbing screen.

The lack of strong continuum absorption distinguishes classical optically selected Seyfert 2 galaxies from the X-ray selected narrow-line galaxies, a group for which there is good evidence of strong absorption (Lawrence and Elvis 1982; Mushotzky 1982). Although Seyfert 2 galaxies and true narrow-line X-ray galaxies share the common property of having only narrow emission lines, evidence suggests that the

nucleus of a classical Seyfert 2 galaxy does not share the property of strong absorption. The fact that Seyfert 2 galaxies (by definition) have brilliant starlike nuclei suggests that light from the nucleus does escape.

A simple model is presented and fitted to the mean ultraviolet to optical emission-line spectrum derived from our data. Photoionization by the inferred power-law continuum, extending well into the X-rays, can reproduce the general features of the observed spectrum with solar abundances, a power-law density distribution, a large range in radii, and a small filling factor. This geometry is consistent with the line-width data for those objects in which [O I] λ6300 is among the sharpest, but does not apply to those in which λ6300 is significantly broader than [S II] $\lambda\lambda$6716, 6731, with their low critical densities. Although these calculations do not strongly confine the chemical composition of the gas, they suggest that the spectrum is consistent with solar or H II region compositions. A comparison between the energy available in ionizing radiation (with a simple power-law continuum) and the emission-line luminosities suggests that additional sources of ionizing radiation, perhaps due to either the presence of hot stars, may exist, or the actual continuum shape may be different from that we assume.

We are grateful to the National Science Foundation for partial support of this research under AST 85-12414 (G. J. F.) and AST 83-11585 (D. E. O.), and NASA for its support through NAG-5-239. Access to archival data was obtained through the facilities of the National Space Science Data Center, and the Regional Data Analysis Facilities at Goddard Space Flight Center. We thank Ronald Stoner for his helpful comments.

APPENDIX

THE PHOTOIONIZATION CALCULATIONS

Calculations are performed with the program most recently described by Netzer and Ferland (1984). The 11 most common elements (H, He, C, N, O, He, Mg, Si, S, Ar, and Fe) are treated, and the equations of statistical and thermal equilibrium are solved in the standard manner (see Williams 1967; Davidson 1972; MacAlpine 1972; Davidson and Netzer 1979). Netzer and Ferland (1984) compare predictions of several such codes and find that the predictions tend to be within 10%–15% of each other. One major recent improvement has been in the treatment of suprathermal secondary electrons; we now use the heating and ionization rates calculated by Shull and Van Steenberg (1985). Since the predictions presented here are not controversial, we concentrate on some of the details germane to the present discussion.

Although recent models are in good agreement, this is not to say that the agreed upon results are completely reliable (this agreement may largely be an artifact of the unified data base resulting from Mendoza's 1983 compilation). In particular, predictions of intensities of third row elements, along with neon, are only tentative because dielectronic recombination through low-lying autoionizing states (often 100–200% of the radiative recombination rate; Storey 1981) is only included for C, N, and O (Nussbaumer and Storey 1983). As a result, the [Ne V]/[Ne III] intensity ratio, along with the red [S II] doublet, are only tentatively predicted.

The solar composition used here is that of Lambert (1978) and Lambert and Luck (1978), with additions from references cited in Pagel and Edmunds (1981). The actual mixture, by number, is He/C/N/O/Ne/Mg/Si/S/Ar/Fe/H = 1000/4.7/0.98/8.3/1.0/0.42/0.43/0.17/0.037/0.33/10^4.

The atomic data used are largely from the compilation by Mendoza (1983). Exception are the collision strengths for [Ne III], which are from Butler and Mendoza (1984). Besides the lack of reliable dielectronic recombination coefficients mentioned above, another serious source of uncertainty concerns the collision strengths used for iron. Collision strengths for lines of Fe III–Fe VI are from Shields (1978), and are estimates obtained by scaling model predictions to observations. As such, they undoubtedly absorb errors due to uncertainties in the thermal and ionization structure of the Shields model. Emissivities of [Fe X] λ6375 and [Fe XIV] λ5303 are calculated with both contributions from both collisional and resonance-fluorescence excitation, as in Osterbrock (1969; however, we use collision strengths from Mason 1975).

The model predicts too strong [Fe II] emission. Atomic data for the Fe^+ ion are presented by Collin-Souffrin *et al.* (1979, 1980), and Wills, Netzer, and Wills (1985) discuss a three-level atom which reproduces their detailed excitation calculations. This "equivalent atom" was used in the present calculations. Uncertainties in the collision strengths may well account for this discrepancy.

REFERENCES

Briggs, S. A., Bokensenberg, A., Carswell, R. F., and Sargent, W. L. W. 1980, *M.N.R.A.S.*, **191**, 665.
Burstein, D., and Heiles, C. 1982, *A.J.*, **87**, 1165.
Butler, K., and Mendoza, C. 1984, *M.N.R.A.S.*, **208**, 17P.
Carroll, T. J., and Kwan, J. 1983, *Ap. J.*, **274**, 113.
Cohen, R. D. 1983, *Ap. J.*, **273**, 489.
Cohen, R. D., and Osterbrock, D. E. 1981, *Ap. J.*, **243**, 81.
Collin-Souffrin, S., Dumont, S., Heidmann, N., and Joly, M. 1980, *Astr. Ap.*, **83**, 190.
Collin-Souffrin, S., Joly, M., Heidmann, N., and Dumont, S. 1979, *Astr. Ap.*, **72**, 293.
Contini, M., and Aldrovandi, S. M. V. 1983, *Astr. Ap.*, **127**, 15.
Costero, R., and Osterbrock, D. E. 1977, *Ap. J.*, **211**, 675.
Daltabuit, E., MacAlpine, G. M., and Cox, D. 1978, *Ap. J.*, **219**, 372.
Davidson, K. 1972, *Ap. J.*, **171**, 213.
Davidson, K., and Netzer, H. 1979, *Rev. Mod. Phys.*, **51**, 715.
deBruyn, A. G., and Sargent, W. L. W. 1978, *A.J.*, **83**, 1257.
DeRobertis, M. M., and Osterbrock, D. E. 1984, *Ap. J.*, **286**, 171.
Fabbiano, G., Miller, L., Trinchieri, G., Longair, M., and Elvis, M. 1984, *Ap. J.*, **277**, 115.
Ferland, G. J., and Netzer, H. 1983, *Ap. J.*, **264**, 105.
Ferland, G. J., and Osterbrock, D. E. 1985, *Ap. J.*, **289**, 105.
Filippenko, A. V., and Halpern, J. P. 1984, *Ap. J.*, **285**, 458.
Fosbury, R. A. E., *et al.* 1982, *M.N.R.A.S.*, **201**, 991.
Gaskell, C. M., and Ferland, G. J. 1984, *Pub. A.S.P.*, **96**, 393.
Halpern, J. P. 1982, Ph.D. thesis, Harvard University.
Halpern, J. P., and Steiner, J. 1983, *Ap. J.* (*Letters*), **269**, L37.
Harrington, J. P., Lutz, J. H., and Seaton, M. J. 1981, *M.N.R.A.S.*, **195**, 21P.
Keel, W. C. 1980, *A.J.*, **85**, 198.
Koski, A. T. 1976, Ph.D. thesis, University of California, Santa Cruz.
———. 1978, *Ap. J.*, **223**, 56.
Kriss, G. A., Canizares, C. R., and Rickert, G. R. 1980, *Ap. J.*, **242**, 492.

Krolik, J., and Vrtilek, J. 1984, *Ap. J.*, **279**, 521.
Lambert, D. L. 1978, *M.N.R.A.S.*, **182**, 249.
Lambert, D. L., and Lucke, R. E. 1978, *M.N.R.A.S.*, **183**, 79.
Lawrence, A., and Elvis, M. 1982, *Ap. J.*, **256**, 410.
MacAlpine, G. M. 1972, *Ap. J.*, **175**, 11.
Malkan, M., and Oke, J. B. 1983, *Ap. J.*, **265**, 92.
Mason, H. E. 1975, *M.N.R.A.S.*, **170**, 651.
Mendoza, C. 1983, in *IAU Symposium 103, Planetary Nebulae*, ed. D. Flower (Dordrecht: Reidel), p. 143.
Mushotzky, R. F. 1982, *Ap. J.*, **256**, 92.
Netzer, H. 1982, *M.N.R.A.S.*, **198**, 589.
———. 1985, *Ap. J.*, **289**, 451.
Netzer, H., and Ferland, G. J. 1984, *Pub. A.S.P.*, **96**, 593.
Neugebauer, G. *et al.* 1980, *Ap. J.*, **238**, 502.
Nussbaumer, H., and Storey, P. 1983, *Astr. Ap.*, **126**, 75.
Osterbrock, D. E. 1969, *Ap. Letters*, **4**, 57.
———. 1981*a*, *Ap. J.*, **246**, 696.
———. 1981*b*, *Ap. J.*, **249**, 462.
———. 1984, *Quart. J.R.A.S.*, **25**, 1.
Osterbrock, D. E., and Miller, J. 1975, *Ap. J.*, **197**, 535.
Osterbrock, D. E., and Parker, R. A. R. 1965, *Ap. J.*, **141**, 892.
Pagel, B. E. J., and Edmunds, M. G. 1981, *Ann. Rev. Astr. Ap.*, **19**, 77.
Pequignot, D. 1984, *Astr. Ap.*, **131**, 159.
Phillips, M. M., Charles, P. A., and Baldwin, J. A. 1983, *Ap. J.*, **266**, 485.
Ptak, R., and Stoner, R. 1973, *Ap. J. (Letters)*, **179**, L89.
Seaton, M. 1979, *M.N.R.A.S.*, **187**, 73P.
Shields, G. A. 1978, *Ap. J.*, **219**, 559.
Shull, J. M., and Van Steenberg, M. E. 1985, *Ap. J.*, **298**, in press.
Stasinska, G. 1984, *Astr. Ap.*, **135**, 341.
Storey, P. J. 1981, *M.N.R.A.S.*, **195**, 27P.
Thuan, T. X. 1984, *Ap. J.*, **281**, 126.
Ulvestad, J. S., and Wilson, A. S. 1983, *A.J.*, **88**, 253.
Veron, P., Lindblad, P., Zuiderwijk, E., and Veron, M. 1980, *Astr. Ap.*, **87**, 245.
Walker, M. F. 1968, *Ap. J.*, **151**, 71.
Weedman, D., and Huenemoerder, D. P. 1985, *Ap. J.*, **291**, 72.
Whittle, M. 1985, *M.N.R.A.S.*, **213**, 33.
Williams, R. E. 1967, *Ap. J.*, **147**, 556.
Wills, B., Netzer, H., and Wills, D. 1985, *Ap. J.*, **288**, 94.
Wu, C. C., Boggess, A., and Gull, T. R. 1983, *Ap. J.*, **266**, 28.
Zamorani, G. *et al.* 1981, *Ap. J.*, **245**, 357.

GARY J. FERLAND: Astronomy Department, The Ohio State University, Colombus, OH 43210

DONALD E. OSTERBROCK: Lick Observatory, University of California, Santa Cruz, CA 95064